THE POTENTIAL OF THE 3-UPU TOPOLOGY FOR TRANSLATIONAL PARALLEL MANIPULATORS AND A PROCEDURE TO SELECT THE BEST ARCHITECTURE FOR A GIVEN TASK

AHMED HACHEM CHEBBI, VINCENZO PARENTI-CASTELLI

Abstract. The 3-UPU three degrees of freedom fully parallel manipulator, where U and P are for universal and prismatic pair respectively, is a very well known manipulator that can provide the platform with three degrees of freedom of pure translation, pure rotation or mixed translation and rotation with respect to the base, according to the relative directions of the revolute pair axes. In particular, pure translational parallel 3-UPU manipulators (3-UPU TPMs) received great attention. However, much work has still to be done to reveal all the features this topology can offer to the designer when different architectures, *i.e.* different geometries, are considered. Therefore, this paper will focus on this type of the 3-UPU manipulators. The paper collects the previous most relevant work done on the 3-UPU TPMs and shows the main results in a coherent general frame. The paper presents new architectures of the 3-UPU TPMs which offer interesting features to the designer. Then, based on a number of indexes, a procedure is proposed that allows the designer to select the best architecture of the 3-UPU TPMs for a given task.

Key words: parallel manipulators, pure translation, architectures, singularity, topology.

1. INTRODUCTION

Recently, parallel manipulators (PMs) with less than three degrees of freedom (DOF) have attracted the attention since many tasks do not require 6-DOF and consequently less complex and cheaper machines are worth to be studied.

In particular 3-DOF PMs have been studied in the last two decades after the Delta robot was proposed in 1988 [1]. Many different topologies have been presented since then with various complexities. Three-DOF PMs of pure translation, rotation and a mixed of rotation and translation have been deeply studied and almost all possible topologies have been presented [2–16]. The influence of the topology on the performances of the manipulator has also been investigated. However, much is still to be said, still keeping the same topology, on

DIN University of Bologna, Department of Industrial Engineering, Italy

Rom. J. Techn. Sci. – Appl. Mechanics, Vol. 58, N^{os} 1–2, P. 5–32, Bucharest, 2013

the influence of the manipulator geometry, *i.e.* of its architecture, which can significantly change the behavior of the manipulator.

An interesting 3-DOF PM is the 3-UPU one, presented by Tsai in [3]. Here U and P are for universal and prismatic kinematic pairs respectively. Normally the P pairs are actuated while the remaining ones are passive. This topology (Fig. 1), that features three serial chains (legs) of type UPU connecting the base with the platform, under certain geometric conditions provides the movable platform with 3 DOF of pure translation with respect to the base. This paper will focus on this family of 3-UPU translational parallel manipulators, hereafter called 3-UPU TPMs.

Since its appearance in [3], the influence of geometry on the 3-UPU TPM performances has been investigated [4, 6, 9, 11, 17, 18, 19], many different architectures presented, and their performances discussed. Moreover, the 3-UPU TPM represented a kind of benchmark mechanism for the study of different type of singularities [5, 6, 9, 11, 14, 17, 18] in parallel manipulators. Nevertheless, further architectures still deserve attention. Indeed, in a recent paper [20], the influence of the location of the legs has been investigated leading to new 3-UPU TPM architectures with interesting features.

The aim of this paper is to present new architectures of the 3-UPU TPM in order to show the potential of the 3-UPU TPM topology on one hand, and on the other hand to propose a new procedure on how a designer can select the best architecture of the 3-UPU TPMs for a given task. In particular, the influence of the orientation of the revolute axes on the base and on the platform respectively, is investigated with special attention to its influence on the singularity loci, and consequently on the manipulator workspace free from singularity, which is one of the major features to pursue in the design of a parallel manipulator. Two new 3-UPU TPM architectures are presented, which exhibit attractive kinematic and static performances. On the other hand, performance indexes are proposed as main tools of a procedure to select the best architecture, also exploiting the definition of singularity that can give useful information for the selection.

2. BACKGROUND ON THE 3-UPU TPM

A schematic of the 3-UPU TPM is shown in Fig. 1. The P joints are actuated. Each U joint comprises two revolute pairs with intersecting and perpendicular axes, centred at point B_i, i = 1, 2, 3, in the base and at point A_i, i = 1, 2, 3, in the platform.

The platform pure translational motion is obtained (and the platform rotation is totally prevented) when the following geometric conditions are satisfied for each leg [3, 4, 6]:

– the axes of the two intermediate revolute pairs are parallel to each other;

– the axes of the two ending revolute pairs are parallel to each other.

What follows in this section refers to a special family of 3-UPU TPM architecture: the one that has the three axes of the revolute pairs in the base/platform in a same plane respectively.

In [20], two architectures of the 3-UPU TPM have been defined. They are here recalled for completeness of presentation.

The first one, defined as architecture 1.A and shown in Fig. 2, occurs when the axes $\mathbf{q}_{1i}$, $i = 1, 2, 3$ and $\mathbf{q}_{4i}$, $i = 1, 2, 3$ of the revolute pairs in the base/platform two-by-two intersect at three points C_i, $i = 1, 2, 3$, which define a plane (see plane π in Fig. 2).

In Fig. 2, only the revolute pairs on the base and the platform are represented for clarity, all other ones are omitted. The same simplification has been adopted for all the subsequent figures of the paper.

The singularity of the manipulator, *i.e.*, when the relationship between a wrench of the external load applied on the platform and the wrench provided by the legs that are related by the Jacobian matrix **J** is no longer a one-to-one relationship, occurs when the determinant K of the Jacobian matrix, $K = \det\mathbf{J}$, vanishes. This condition is given by [6]

$$\left[\mathbf{s}_1.\left(\mathbf{s}_2 \times \mathbf{s}_3\right)\right].\left[\mathbf{u}_1.\left(\mathbf{u}_2 \times \mathbf{u}_3\right)\right] = 0\,, \tag{1}$$

where $\mathbf{s}_i$, $\mathbf{u}_i$, $i = 1, 2, 3$ (Fig. 1), are respectively the unit vector of the i^{th} leg A_iB_i and the unit vector orthogonal to the cross link of the U joint in the i^{th} leg on the base/platform.

A system of reference S_b fixed to the base with origin O_b (the centre of the circle with radius b defined by the points B_i, $i = 1, 2, 3$) is chosen. Axes x and y are on the plane π, with x axis through point B_1, z axis is pointing upward from the base to the platform, while y axis is taken according to the right hand rule.

Singularities occur when:

– all unit vectors $\mathbf{s}_i$ become coplanar. This occurs when point O_p (center of the circle with radius p defined by the points A_i, $i = 1, 2, 3$) and origin of the reference system S_p fixed to the platform with x axis through point A_1 and z axis is pointing upward from the base to the platform, while y axis obtained according to the right hand rule lies on the plane π. This plane corresponds to $z = 0$ in S_b;

– two out of three unit vectors $\mathbf{u}_i$ become parallel. This occurs when points A_i and A_j ($i = 1, 2, 3$, $j = 1, 2, 3$, $i \neq j$) belong respectively to the two planes δ_i and δ_j orthogonal to the base and containing respectively $\mathbf{q}_{1i}$ and $\mathbf{q}_{1j}$. In this position also $\mathbf{q}_{4i}$ and $\mathbf{q}_{4j}$, which are always parallel to $\mathbf{q}_{1i}$ and $\mathbf{q}_{1j}$, belong to the planes δ_i and δ_j.

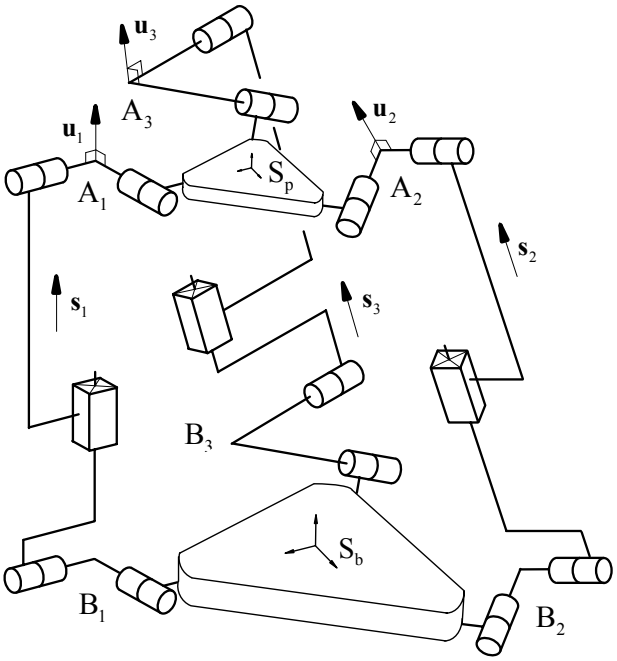

Fig. 1 – The 3-UPU TPM.

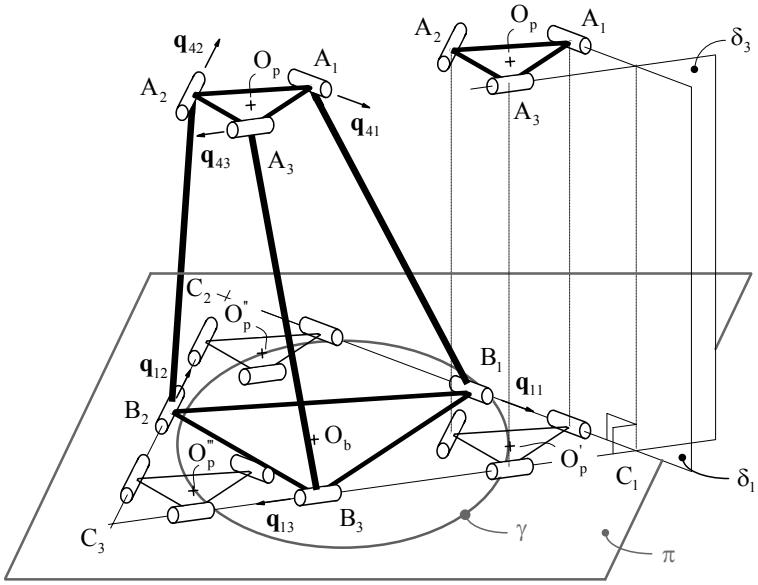

Fig. 2 – Singularity loci for the architecture 1. A of the 3-UPU TPM.

This condition is represented in Fig. 2 when vectors $\mathbf{q}_{41}$ and $\mathbf{q}_{43}$ project on $\mathbf{q}_{11}$ and $\mathbf{q}_{13}$ respectively. In this position, point O_p of the platform projects on point O_p' in the base plane π. Similar conditions occur when considering vectors $\mathbf{q}_{41}$ and $\mathbf{q}_{42}$, and vectors $\mathbf{q}_{42}$ and $\mathbf{q}_{43}$, which lead to define similar points O_p' and O_p'' in the base plane π. Analytically, it can be proved that a singularity locus is a right cylinder Γ [4], with circular directrix γ and axis coincident with the z axis of S_b. Therefore, conversely, once the points O_p', O_p'' and O_p''' are defined, the circle γ is defined and the cylinder Γ is defined too. The three points can be easily found by geometrical inspections, thus representing a simple and efficient method to easily find the cylinder Γ. This cylinder has radius $r = 2(b–p)$.

– the base and the platform have the same size. In this case all $\mathbf{s}_i$ $i = 1, 2, 3$, become mutually parallel for any position of the platform and, according to the Eqn.(1), the manipulator is in a singular position and the manipulator is structurally singular [4, 6, 11].

The second architecture (architecture 1.B) is obtained by disconnecting the platform of the architecture 1.A from the legs and rotating it 180 degrees about the z axis of S_b, then again connecting the legs to the same corresponding platform revolute pairs. This makes the three legs intersect at one point as shown in Fig. 3. This is a practical drawback. However, manufacturing solutions can overcome it. Indeed, some efficient manufacturing solutions are presented in [20] to avoid the collision of the legs.

The singularity loci of this architecture correspond respectively to (i) the plane π ($z = 0$ in S_b); (ii) the cylinder with axis z of S_b and with radius $r = 2(b+p)$, and (iii) the whole three dimensional Cartesian workspace when the base and the platform have the same size. Systems S_b and S_p are defined as in the previous 3-UPU TPM architecture.

It is worth noting that, for the same size of the base and the platform, the 3-UPU TPM with architecture 1.B has a larger cylinder of singularity than that with architecture 1.A, thus it allows a larger workspace free from singularity inside the cylinder.

3. NEW ARCHITECTURES OF THE 3-UPU TPM

This section presents new architectures of the 3-UPU TPM. 3-UPU TPMs can be classified in two main families: 3-UPU TPM with planar base and with skew base: named as planar and skew architectures for brevity.

Planar architectures have the three revolute joint axes connecting the base/platform with the leg on a plane (for the base, plane π in Fig. 2), while the skew architectures have these three axes not belonging to a same plane but they are skewed.

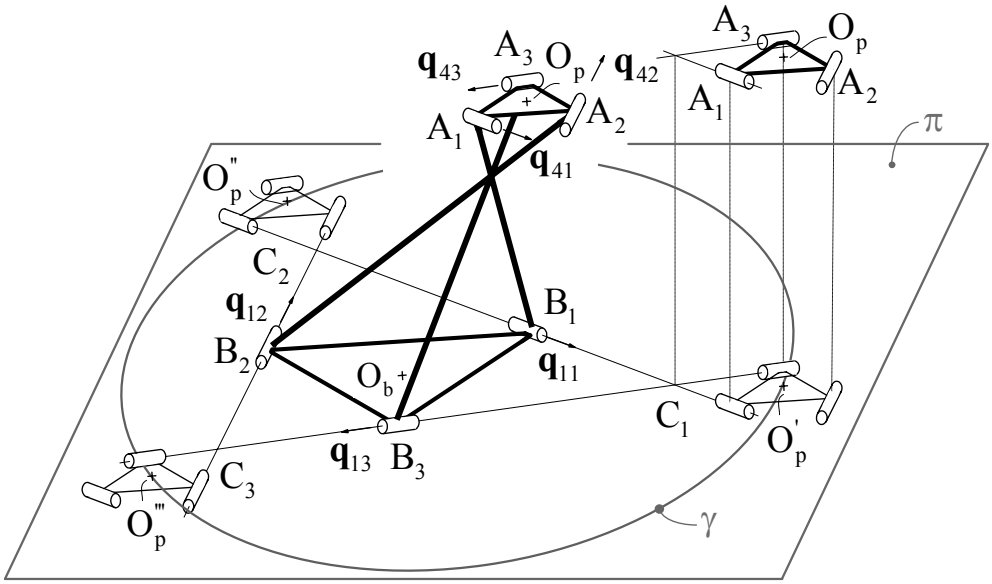

Fig. 3 – Singularity loci for the architecture 1.B of the 3-UPU TPM.

3.1. PLANAR ARCHITECTURES

In this section, two new architectures of the 3-UPU TPM are presented. The first architecture (defined as architecture 2.A) is obtained by taking two axes of the base/platform revolute pairs out of the three mutually parallel. Figure 4 shows a case with the unit vectors $\mathbf{q}_{11}$ and $\mathbf{q}_{13}$ mutually parallel and orthogonal to the unit vector $\mathbf{q}_{12}$ of the third axis. The centers of the universal joints in the base/platform are chosen so as to have the angle between the vectors O_bB_i and O_bB_{i+1}, $i = 1, 2, 3$, and respectively the vectors O_pA_i and O_pA_{i+1}, $i = 1, 2, 3$, equal to $2\pi/3$. S_b is defined as in the previous architectures.

Singularity loci: similarly to the two previous cases (architectures 1.A and 1.B) also this new architecture 2.A when $b = p$ is structurally singular. For $b \neq p$, the Eqn.(1) is satisfied when: (i) the unit vectors $\mathbf{s}_i$ become coplanar and belong to the plane π ($z = 0$), and (ii) two out of three unit vectors $\mathbf{u}_i$ become parallel. This latter condition occurs when A_i and A_j ($i = 1, 2, 3$, $j = 1, 2, 3$, $i \neq j$) belong respectively to the two planes orthogonal to the base and containing respectively $\mathbf{q}_{1i}$ and $\mathbf{q}_{1j}$ (defined as in the previous 3-UPU TPM architectures). This condition is shown in Fig. 4 for the position of the platform when point O_p projects on O_p'. A similar position occurs when point O_p projects on O_p''.

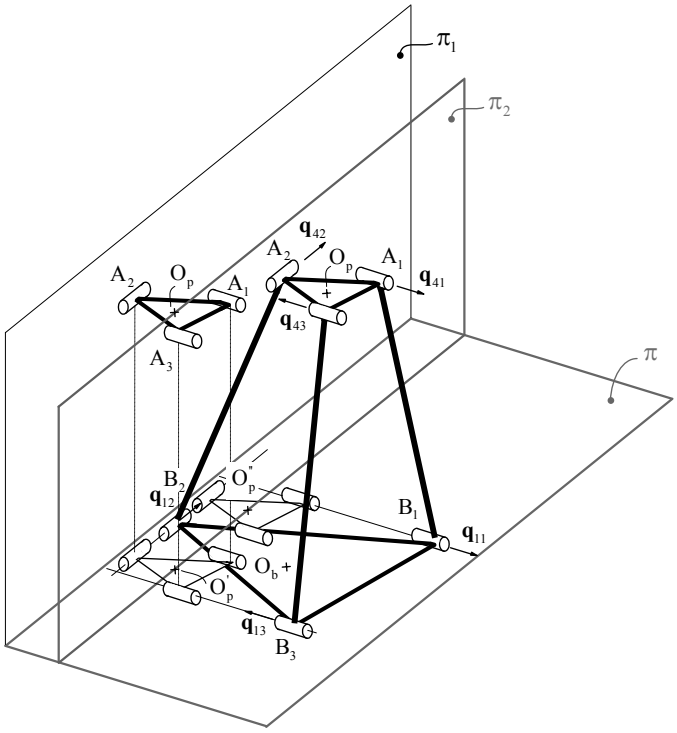

Fig. 4 – Singularity loci for the architecture 2.A of the 3-UPU TPM.

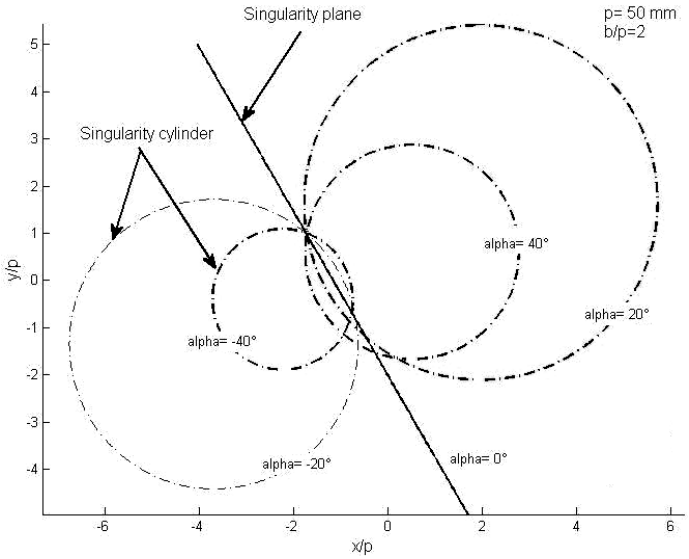

Fig. 5 – Singularity cylinder and singularity plane of the 3-UPU TPM.

The third point, analogous to O_p''' of the previous architectures goes to infinite since $\mathbf{q}_{13}$ and $\mathbf{q}_{11}$ are parallel. Therefore, the circle γ, directrix of the singularity cylinder Γ, becomes a line passing through points O_p' and O_p''. As a consequence, the singularity cylinder becomes the plane π_2, orthogonal to π and passing through the two points O_p' and O_p''. The equation of this plane can be represented as follows:

$$y = \frac{\lambda_2}{\kappa_2}\left(x - (b-p)\cos\left(\frac{2\pi}{3}\right)\right) + (b-p)\sin\left(\frac{2\pi}{3}\right), \quad \forall z \in \mathbb{R}, \tag{2}$$

where κ_2 and λ_2 are respectively the x and y components of the vector $\mathbf{q}_{12}$ in the reference system S_b, and x, y and z are the coordinates of the point O_p in the reference system S_b.

Let α be the angle between the axes of the two revolute pairs connecting the first and the third leg to the base, *i.e.* the angle between the unit vectors $\mathbf{q}_{11}$ and $\mathbf{q}_{13}$, $\alpha = \left(\widehat{\mathbf{q}_{11}, \mathbf{q}_{13}}\right)$. In Fig. 4, α is 180 degrees. Figure 5 that reports the intersection of the singularity loci with the plane π (x, y plane of S_b) for different values of the angle α shows the changing of the singularity loci from a cylinder to a plane according to the value of the angle α, *i.e.*, when the value of the angle α is equal to zero or 180 degrees, the singularity loci corresponds to a plane. If this condition does not occur, the singularity loci correspond to a cylinder.

It is worth noting that 3-UPU TPMs with architecture 2.A have a workspace consisting of a volume, plane π_2 apart, free from singularity.

Similarly to what was done for the transition from architecture 1.A to the architecture 1.B (changing the location of the legs), a further 3-UPU TPM architecture can be devised. Indeed, by disconnecting the platform from the legs, rotating it 180 degrees about z axis, then reassembling it to the same corresponding platform revolute pairs, still keeping the same direction of the base revolute pairs, a new architecture defined as architecture 2.B can be found as shown in Fig. 6. This architecture leads to the intersection of the three legs at one point.

By the same procedure as in the previous architectures, the singularity loci of this architecture is found and it corresponds to the two planes π and π_2'.

The equation of π_2' can be represented analytically as follows:

$$y = \frac{\lambda_2}{\kappa_2}\left(x - (b+p)\cos\left(\frac{2\pi}{3}\right)\right) + (b+p)\sin\left(\frac{2\pi}{3}\right), \quad \forall z \in \mathbb{R}, \tag{3}$$

where κ_2 and λ_2 are respectively the x and y components of the vector $\mathbf{q}_{12}$ in the reference system S_b, which is defined as in the previous 3-UPU TPMs architectures.

Similarly to the previous case (architecture 2.A), it is worth noting that 3-UPU TPMs with architecture 2.B have a workspace consisting of a volume, plane π_2 apart, free from singularity.

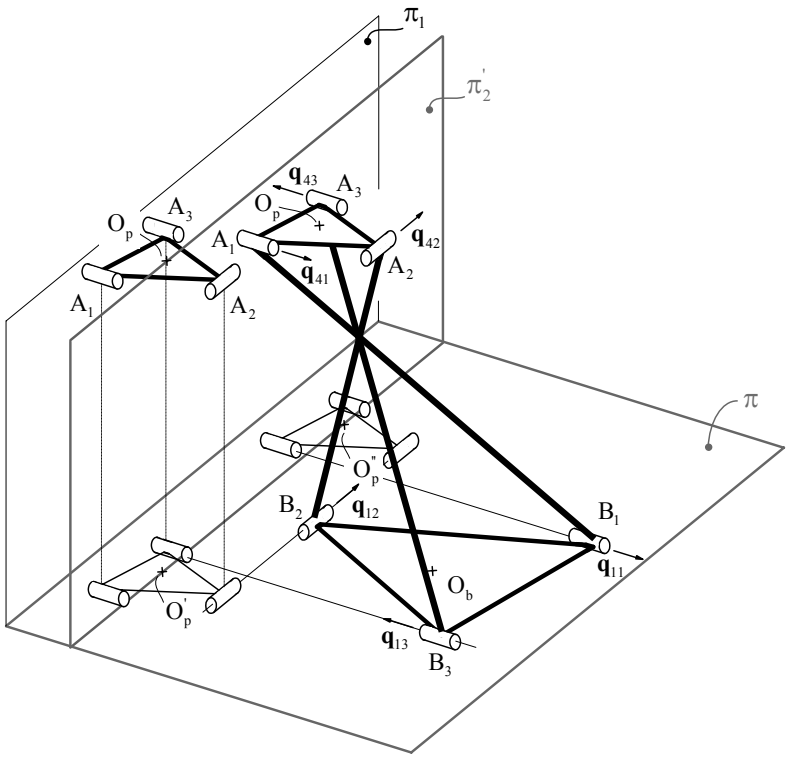

Fig. 6 – Singularity loci for the architecture 2.B of the 3-UPU TPM.

3.2. SKEW ARCHITECTURES

By considering a skew relative position of the axes of the base/platform revolute joints, new architectures were found and presented in [20]. Their schematics are reported in Figs. 7–10. In this section a complete (original) study on the singularity loci is presented.

For the first architecture (Fig. 7) defined as architecture 3.A, the axes of two revolute pair on the base are on the plane π. The axis of the third revolute pair is orthogonal to the plane π as shown in Fig. 7. The singularity loci [20] correspond to:

– the plane π;

– the structural singularity, *i.e.*, the base and the platform have the same size;

– three lines δ_{ij}, $i = 1, 2, j = 2, 3, i \neq j$, which represent the locus of the reference point O_p when, according to the method reported in section 2, two axes of

the revolute pairs of the platform ($\mathbf{q}_{4i}$, $\mathbf{q}_{4j}$) projects on the two corresponding axes of the base ($\mathbf{q}_{1i}$, $\mathbf{q}_{1j}$), providing the projection direction is along the unit vector $\mathbf{v}_{ij}$ of the shortest distance among the two axes. A geometrical inspection shows that the lines δ_{23} and δ_{13} are on the plane π. While the line δ_{12} is orthogonal to the plane π.

In [20] only some information on the singularities is reported based on geometric inferences, then a complete study is reported here based also on analytical tools.

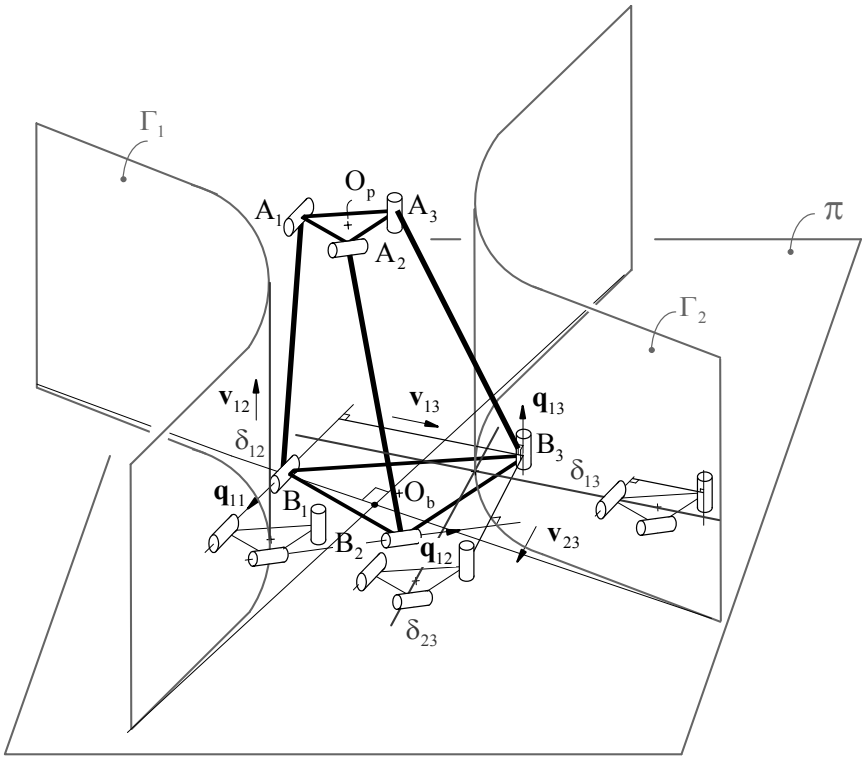

Fig. 7 – Singularity loci for the architecture 3.A of the 3-UPU TPM.

By substituting the expression of the vectors $\mathbf{s}_i$ and $\mathbf{u}_i$ in Eqn. (1) and equating the numerator to zero, it is possible to find:

$$z\left(Ax^2 + Bxy - Ay^2 + Dx + Ey + F\right) = 0, \tag{4}$$

where x, y and z are the coordinates of the point O_p in the system S_b and the coefficients A, B, D, E and F depend on the x and y coordinates of the point O_p in the system S_b, on the direction of the revolute joint of the base and on the radii b, p (the full expression of A, B, D, E and F are reported in Annex A).

Equation (4) is satisfied when:

$$\begin{cases} z = 0 \\ Ax^2 + Bxy - Ay^2 + Dx + Ey + F = 0, \quad \forall z \in \mathbb{R}, \end{cases} \tag{5}$$

Thus, the singularity loci correspond to the plane π ($z = 0$) and, from the second equation of Equations (5), to two surfaces Γ_1 and Γ_2, which are ruled surfaces (represented in Fig. 7) that intersect the plane π on a rectangular hyperbola.

For the second architecture, defined as architecture 4.A, two axes of the revolute pairs on the base are mutually parallel and belong to the plane π, while the third one is orthogonal to the plane π as shown in Fig. 8.

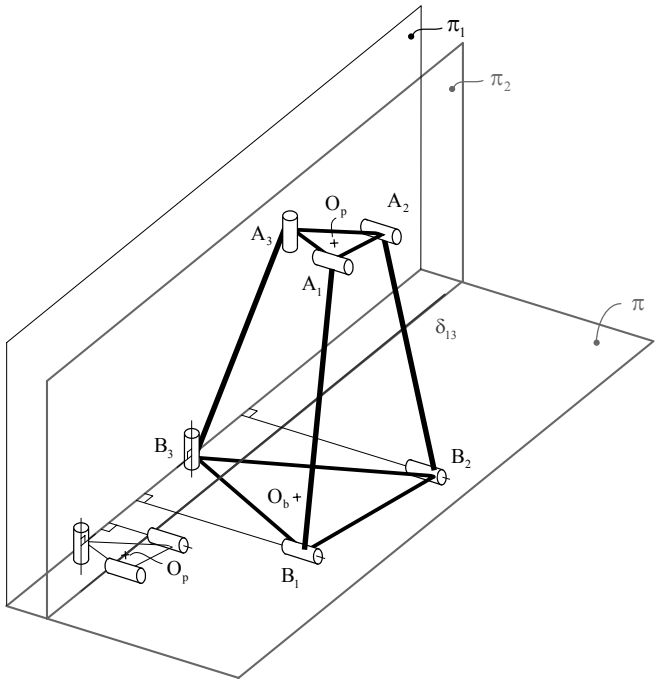

Fig. 8 – Singularity loci for the architecture 4.A of the 3-UPU TPM.

The singularity loci correspond to the plane π and to a line δ_{13} (δ_{23}) (locus of the platform reference point) on this plane obtained by the projection of the axes of the two revolute pairs $\mathbf{q}_{11}$ and $\mathbf{q}_{13}$ ($\mathbf{q}_{12}$ and $\mathbf{q}_{13}$) of the platform on the two corresponding axes of the base in the direction orthogonal to these two axes. It can be concluded that the singularity loci is the plane π [20].

Likewise the previous architecture, by substituting the expression of the vectors $\mathbf{s}_i$ and $\mathbf{u}_i$ in Eqn. (1) and equating the numerator to zero, an equation similar to Eqn. (4) is obtained, but in this case, the coefficients A and B are equal to zero, therefore Eqn. (4) becomes:

$$z\left(Dx + Ey + F\right) = 0\,. \tag{6}$$

Thus, the singularity loci correspond to two planes: the plane π ($z=0$) and the plane π_2 (orthogonal to π and containing the line δ_{13} as shown in Fig. 8) which has the following equation:

$$y = -\frac{\left(D\,x + F\right)}{E}, \qquad \forall z \in \mathbb{R}. \tag{7}$$

Similarly to what was done for the transition from architecture 1.A to the architecture 1.B (changing the location of the legs), a further 3-UPU TPM architecture can be devised. Indeed, by disconnecting the platform from the legs of the architectures 3.A and 4.A respectively, rotating it 180 degrees about z axis, then reassembling it to the same corresponding platform revolute pairs, still keeping the same direction of the base revolute pairs, two new architectures defined as architecture 3.B and architecture 4.B, can be found as shown in Fig. 9 and Fig. 10. These architectures lead to the intersection of the three legs at one point.

Analogously to the architectures 3.A and 4.A, the singularity loci of the architecture 3.B is the plane π and two surfaces Γ_1' and Γ_2', and for the architecture 4.B the two planes π and π_2'.

4. PROCEDURE TO SELECT THE BEST 3-UPU ARCHITECTURE FOR A GIVEN TASK

In this section, a procedure to select the best 3-UPU TPM architecture for a given task among a number of 3-UPU TPM architectures is presented. In particular, the task is to have a given Cartesian workspace of the platform free from singularities. It is worth noting that the proposed procedure can be applied (in general) to any 3-DOF manipulator. The core of the procedure is the definition of a number of geometrical indices which will be used to select the best architecture of the manipulator according to the task. This procedure is composed of five main steps.

Before proceeding to the first step, the meaning of security index K_d is recalled. With reference to Eqn. (1), $\det\mathbf{J} = K_d$ represents a closed surface in the Cartesian space inside/outside of which K is smaller/greater than a given value of K, K_d [4, 13]. Here, K is re-defined as security index, since it represents how far from the singularity ($K = 0$) the manipulator configuration is.

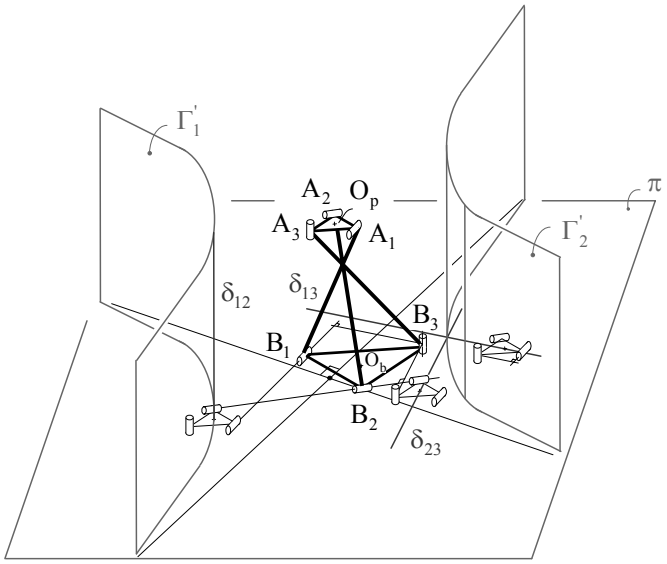

Fig. 9 – Singularity loci for the architecture 3.B of the 3-UPU TPM.

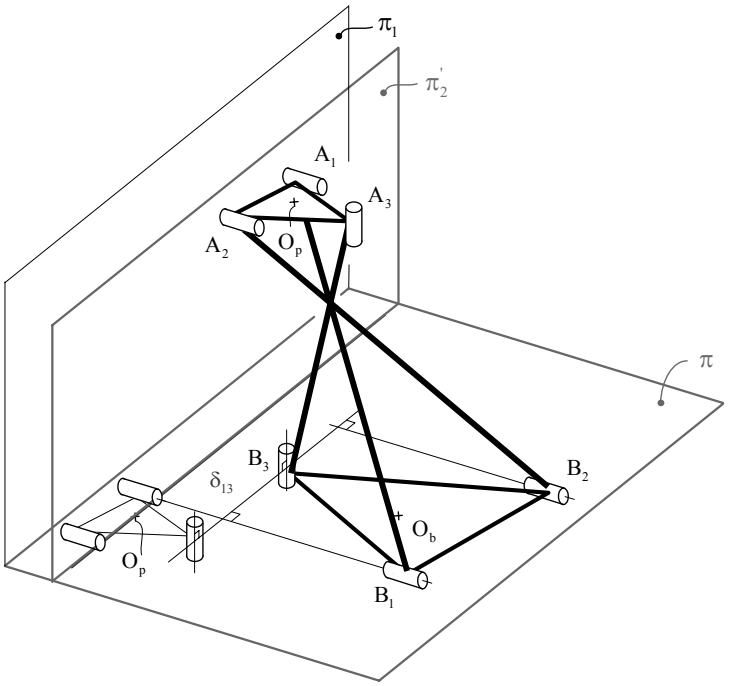

Fig. 10 – Singularity loci for the architecture 4.B of the 3-UPU TPM.

First step: the given workspace is put inside a sphere S or inside an easy to define surface. Then the sphere is considered as the given workspace. The sphere is placed inside a surface with $K \geq K_d$, where K_d is a given security index. This guarantees that the manipulator has $K \geq K_d$ for all points of the sphere. It is worth noting that, in general, the value of K, which stems from Eqn.(1), is between 0 and 1.

The second step is the definition of an objective function that the manipulator has to satisfy. The objective function can be defined by a proper weighted selection of one or more indices, each of them related to a specific property of the manipulator, such as size, kinematic manipulability, performance index, forces and moments applied on each leg, stiffness, and volume of the closed surface $K = K_d$. These indexes are taken from the literature but some of them are reported for clarity in Annex B.

The third step is to compute the selected indexes for a section W of the given workspace. The computation should indeed be performed on the whole workspace. However, this is a time consuming step that is not worth in most cases, thus, quite often, it can be avoided by limiting the computation to a significant subset of the workspace; for instance, a chosen section of it. As a rule of thumb, the chosen section may contain the center of the sphere and is parallel to the plane π.

The fourth step is to normalize the n selected indexes computed in the previous step, in order to find a criterion of comparison, as follows:

$$T_i = \frac{\int_{\mathrm{W}} t_i \mathrm{d}W}{\int_{\mathrm{W}} \mathrm{d}W}, \qquad i = 1, ..., n, \tag{8}$$

where t_i and n are respectively the i^{th} index value and the number of indexes, W is the selected subset of the workspace and T_i is the normalized i^{th} index value. There is no closed-form solution for Eqn. (8), then the integral of the i^{th} index, is calculated numerically, which can be approximated by a discrete sum:

$$T_i \approx \frac{1}{N_v} \sum_{v \in \mathrm{W}} t_i, \qquad i = 1, ..., n, \tag{9}$$

where v is one of the N_v points, which are uniformly distributed in W.

The previous four steps have to be completed for all the available investigated architectures.

The fifth step is to select the 3-UPU TPM architecture which best satisfies the selected objective function (see second step above).

It is worth noting that the proposed procedure is not an iterative procedure, although it could be organized as such. Indeed, the five steps are all straightforward and lead to the selection of the best architecture among the ones considered. The best one provides a workspace free from singularities and in addition satisfies the objective function represented by either one single index or a weighted average of a number of them.

5. CASE STUDY

This section reports the application of the procedure presented in the previous section for the selection of the best architecture of the 3-UPU TPMs among the four ones (1.A, 1.B, 2.A, 2.B) reported in sections 2 and 3.1. The best architecture is selected based on each individual index taken as an objective function (a proper selection of weighted indexes as objective function would provide of course different results). The given data are: the radius p=45 mm; the security index K_d = 0.6; the diameter d of the sphere S, d = 200 mm; and the same for each leg: the offset e = 30 mm; the external radius R_{ext}= 8 mm; the internal radius R_{int}=5.5 mm; Young and Coulomb modules (Aluminium) E = 69 000N/mm^2; G = 26 000 N/mm^2.

The directions of the revolute pairs on the base, measured in S_b, are taken as:

• architectures 1.A and 1.B: $\mathbf{q}_{1i}$ (i = 1, 2, 3) are along the line tangent to the circle defined by points B_i (i = 1, 2, 3).

• architectures 2.A and 2.B: $\mathbf{q}_{11}$=$\mathbf{q}_{13}$=[0.5 –0.866 0]^T; $\mathbf{q}_{12}$=[0.866 0.5 0]^T

In order to avoid the collision of the legs for the architectures 1.B and 2.B, the second of the three manufacturing solutions presented in [20] has been chosen. The value of the offset will be used only for these architectures in order to avoid the leg collision.

In the following subsections, according to the definition (8), the normalized indexes of kinematic manipulability TKM, of performance index TPI, of force TF, of moment TM, and of stiffness T_{sfi}, i = 1, 2, 3, 4, are computed and the final best architecture is chosen according to each of them taken as objective function.

5.1. SIZE OF THE MANIPULATOR

By applying the procedure presented in [13], the coordinates of the center of the sphere S expressed in S_b in [mm] for the architectures (1.A, 1.B) and (2.A, 2.B) are respectively (0,0,177.39) and (50,–90,218.125). Then, the computed rate b/p, taken as size index, is given in Table 1 for each architecture. Therefore, the architecture 1.B is the best one according to the size of the manipulator criterion.

Table 1

The value of b/p for each architecture

Architecture	1.A	1.B	2.A	2.B
b/p	5.81	3.81	7.25	5.25

5.2. KINEMATIC MANIPULABILITY

The distribution of the kinematic manipulability KM, as defined in [24], of a 3-UPU TPMs in the section W of the workspace (section W at z = 177.39 mm and z = 218.125 mm respectively for the architectures (1.A, 1.B) and the architectures (2.A, 2.B)) is shown in Fig. 11. This distribution is the same for the architectures 1.A and 1.B (respectively 2.A and 2.B). Indeed, architectures 1.A and 1.B (respectively 2.A and 2.B) have the same manipulability since the manipulability depends on K = det**J**, which is a function of the directions of the unit vectors $\mathbf{s}_i$ and $\mathbf{u}_i$, i = 1, 2, 3, that are the same for these two architectures for the same platform position. Then, the corresponding values of the normalized kinematic manipulability index, T_{KM}, are computed in Table 2. The best architecture corresponds to the maximum value of T_{KM}. According to the values of Table 2, the architectures (1.A, 1.B) are better than the architectures (2.A, 2.B).

5.3. PERFORMANCE INDEX

According to [21], the characteristic length L is chosen in order to minimize the condition number a of the manipulator *via* an optimization procedure. The value of a with respect to the characteristic length L in every position of the workspace and for all the four architectures of the manipulator is decreasing. Hence, there is no minimum of the condition number. However, it is possible to proceed in another way [22] by taking L as the average magnitude of vectors O_pA_i, i = 1, 2, 3. Thus, the values of the normalized performance index, T_{PI}, based on [22, 23] and taking into account [25], are computed and reported in Table 3. According to the values of Table 3, the best architecture is the architecture 1.A.

5.4. FORCES AND MOMENTS APPLIED ON EACH LEG OF THE MANIPULATOR

By using the rate b/p given in Table 1, it can be inferred that the directions of the three legs of the manipulator are the same for the architectures 1.A and 1.B (respectively 2.A and 2.B) as schematically shown in Fig. 12. Thus, the values of the normalized force index, T_F, reported in Table 4 are the same for the architectures 1.A and 1.B (respectively 2.A and 2.B).

Table 2

The value of T_{KM} for each architecture

Architecture	1.A	1.B	2.A	2.B
T_{KM}	0.9034	0.9034	0.7845	0.7845

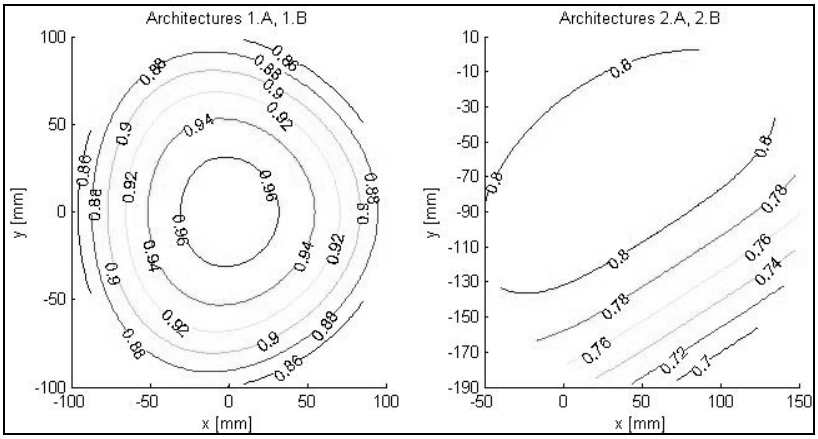

Fig. 11 – Manipulability distribution of a 3-UPU TPM in the section W of the workspace.

The best architecture corresponds to the minimum value of T_F (minimum of the forces applied on each leg). According to the values of Table 4, the architectures (1.A, 1.B) are better than the architectures (2.A, 2.B).

For the values of the normalized moment, T_M, the characteristic length L is introduced. According to [21], the characteristic length is chosen in order to minimize the square root of the determinant of the product of $\mathbf{M}_2$ (see Annex B) by its transpose *via* an optimization procedure. The value of this determinant with respect to L in every position of the workspace and for each architecture of the manipulator is decreasing. However, another way [22] can be adopted by taking L as the average magnitude of vectors O_pA_i, $i = 1, 2, 3$.

Thus, the value of T_M is computed and reported in Table 4. The best architecture corresponds to the minimum value of T_M (minimum of the moment applied on each leg). According to the values of Table 4, the architecture 2.A is the best.

5.5. STIFFNESS OF THE 3-UPU TPM

The values of the normalized stiffness index, T_{sfi}, $i = 1, 2, 3, 4$, are computed and reported in Table 5. According to T_{sf2}, T_{sf3}, and T_{sf4} (Annex B), the architecture 1.B is the best. On the contrary, if the comparison is done according to T_{sf1}, the architecture 1.A is the best.

Table 3

The value of T_{PI} for each architecture

Architecture	1.A	1.B	2.A	2.B
T_{PI} [10^{-5}]	4.82	3.77	2.71	1.82

Table 4

The value of T_F and T_M for each architecture

Architecture	1.A	1.B	2.A	2.B
T_F	1.066	1.066	1.102	1.102
T_M	1.874	2.167	1.765	2.096

Table 5

The value of T_{sfi}, i = 1, 2, 3, 4, for each architecture

Architecture	1.A	1.B	2.A	2.B
T_{sf1} [$N^2/mm^2 \cdot 10^{12}$]	15.04	10.06	6.73	5.32
T_{sf2} [$N^2/rd^2 \cdot 10^{14}$]	6.74	$1.24 \cdot 10^4$	2.52	$5.32 \cdot 10^3$
T_{sf3} [$N^2 \cdot 10^6$]	1.97	$7.23 \cdot 10^{11}$	0.92	$3.02 \cdot 10^{11}$
T_{sf4} [$N^2mm^2/rad^2 \cdot 10^{20}$]	6.58	$8.54 \cdot 10^2$	3.07	$3.09 \cdot 10^2$

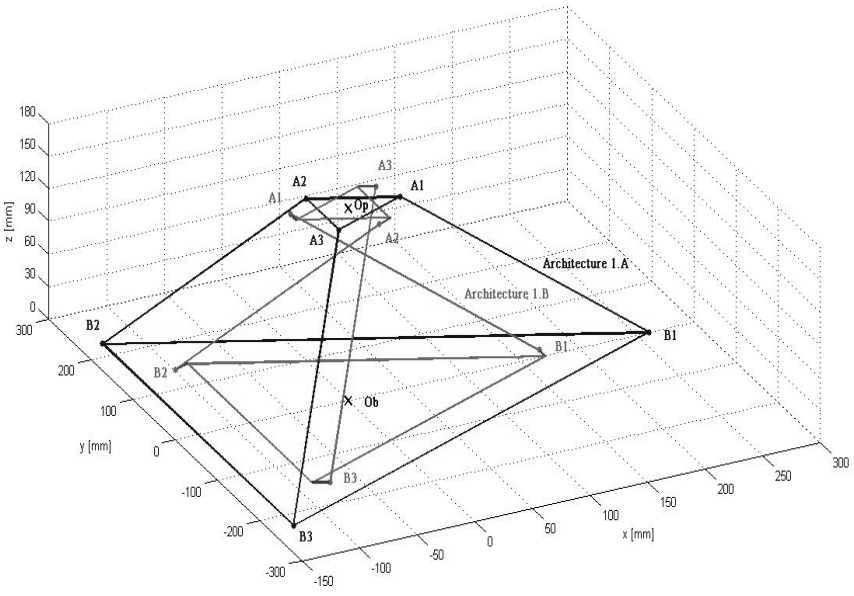

a

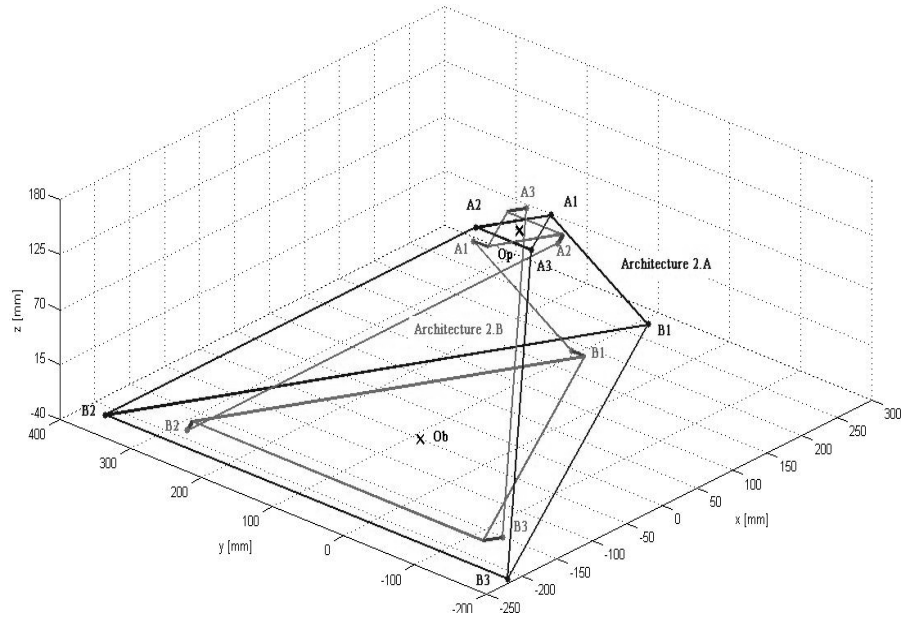

b

Fig. 12 – Architectures 1.A and 1.B (a); and 2.A and 2.B (b), of the 3-UPU TPM for the correspondent rate b/p in a position of the workspace.

5.6. VOLUME OF THE CLOSED SURFACE K = KD

The volume of the closed surface $K = K_d$ corresponding to the architectures 2.A and 2.B is greater than the ones corresponding to the architectures 1.A and 1.B. Figure 13 shows a section of these two volumes . Then, it can be concluded that the architectures 2.A and 2.B are better than the other two architectures.

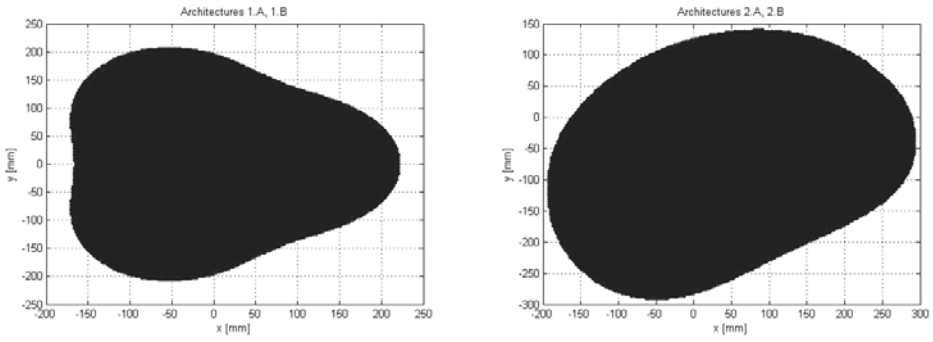

Fig. 13 – Section (z = 200 mm) of the closed surface $K = K_d$, respectively for the (1.A and 1.B) and the (2.A and 2B) architectures of the 3-UPU TPM.

6. CONCLUSION

This paper recalls the most relevant features of the 3-UPU TPMs, a very well known 3-DOF translational manipulator presented in the literature in the late nineties by Tsai [3].

The investigation on the influence that some geometric parameters of the manipulators, such as the direction of the base and platform revolute axes, have on the singularity surfaces and, consequently, on the performances of the manipulator, made it possible to devise new manipulator architectures, which exhibit interesting kinematic and static features showing the potential of the 3-UPU topology.

A procedure to select the best 3-UPU TPM architecture among a number of them for a given task has been presented. The procedure is based on a proper selected number of performance indexes taken from the literature.

Finally, a case study is reported that shows the efficiency of the proposed procedure on one hand and highlights the potential of the 3-UPU TPM topology on the other hand.

Acknowledgements. The financial support of MIUR, INAIL, and BRAVO project is gratefully acknowledged.

ANNEX A

The expressions of A, B, D, E and F are the following:

$$A = \kappa_1\kappa_2\left(\lambda_1^2 + \lambda_2^2\right) - \lambda_1\lambda_2\left(\kappa_1^2 + \kappa_2^2\right), \tag{A.1}$$

$$B = 2\left(\lambda_1^2\kappa_2^2 - \kappa_1^2\lambda_2^2\right), \tag{A.2}$$

$$D = -(b-p)\left(\frac{\kappa_1\left(\lambda_1^2 + \lambda_2^2\right)\left(\sqrt{3}\kappa_1 + \kappa_2\right)}{2} + \lambda_1\lambda_2\left(\kappa_1^2 + \kappa_2^2\right)\right), \tag{A.3}$$

$$E = -(b-p)\left(\frac{\sqrt{3}\kappa_1\kappa_2\left(\lambda_1^2 + \lambda_2^2\right)}{2} + \frac{3\kappa_2^2\lambda_2^2}{2} + \frac{\lambda_1^2\kappa_2^2}{2} + \kappa_1^2\lambda_2^2\right), \tag{A.4}$$

$$F = -(b-p)^2\left(\frac{\left(\lambda_1^2 + \lambda_2^2\right)\left(2\kappa_1\kappa_2 + 3\sqrt{3}\kappa_2^2 + \sqrt{3}\kappa_1^2\right)}{4} + \lambda_1\lambda_2\left(\kappa_1^2 + \kappa_2^2\right)\right), \tag{A.5}$$

where κ_1, λ_1, κ_2 and λ_2 are respectively the x and y components of the vectors $\mathbf{q}_{11}$ and $\mathbf{q}_{12}$ in the system S_b.

ANNEX B

Normalized forces and moments indexes, T_F and T_M

In this section, indexes for both forces and moments applied on each leg of the manipulator are defined.

In order to obtain the full 6×6 matrix that maps the platform wrench to the external load applied on the platform, the static equilibrium equations are given by [19]:

$$\begin{bmatrix} f_1 & f_2 & f_3 & m_1 & m_2 & m_3 \end{bmatrix}^{\mathrm{T}} = \begin{bmatrix} \mathbf{S}^{-1} & \mathbf{0} \\ -\mathbf{U}^{-1}\mathbf{R}\mathbf{S}^{-1} & \mathbf{U}^{-1} \end{bmatrix} \begin{bmatrix} \mathbf{F} \\ \mathbf{M} \end{bmatrix}, \tag{B.1}$$

where f_i, i = 1, 2, 3, and m_i, i = 1, 2, 3 respectively are the force and moment acting on the i^{th} leg,

$$\mathbf{S} = \begin{bmatrix} \mathbf{s}_1 & \mathbf{s}_2 & \mathbf{s}_3 \end{bmatrix}, \tag{B.2}$$

$$\mathbf{R} = \begin{bmatrix} \mathbf{r}_{\mathrm{p}1} \times \mathbf{s}_1 & \mathbf{r}_{\mathrm{p}2} \times \mathbf{s}_2 & \mathbf{r}_{\mathrm{p}3} \times \mathbf{s}_3 \end{bmatrix}, \tag{B.3}$$

$$\mathbf{U} = \begin{bmatrix} \mathbf{u}_1 & \mathbf{u}_2 & \mathbf{u}_3 \end{bmatrix}, \tag{B.4}$$

with $\mathbf{r}_{\mathrm{p}i} = \overrightarrow{O_p A_i}$, i = 1, 2, 3; $\mathbf{F}$ is the resultant force of the external load applied to the platform at point O_p and $\mathbf{M}$ is the resultant moment with respect to point O_p of the external load applied to the platform.

The determinant of the matrix 6×6 given by Eqn.(B.1) cannot be taken as an index because the components of this matrix do not have the same units [25]. One possible solution, is the partition of this matrix in two matrices (3×6) $\mathbf{M}_1$ and $\mathbf{M}_2$.

Now, the force index, T_F, is taken as the square root of the determinant of the product of $\mathbf{M}_1$ by its transpose. The same strategy is chosen for the moment index, T_M, (the square root of the determinant of the product of $\mathbf{M}_2$ by its transpose) taking into account the characteristic length [21] in order to make the matrix $\mathbf{M}_2$ dimensionless.

Stiffness indexes of the 3-UPU TPM

The stiffness indexes, sf_i, i = 1, 2, 3, 4, are proposed in [26] and their major features are reported for clarity in the following. These indexes are based on the

stiffness matrix **H** that provides the relation between a wrench, $[\mathbf{F}\ \mathbf{M}]^T$, applied at the reference point O_p of the platform and the displacement, $[\mathbf{t}\ \mathbf{r}]^T$, of the platform itself:

$$\begin{bmatrix} \mathbf{F} \\ \mathbf{M} \end{bmatrix} = \mathbf{H} \begin{bmatrix} \mathbf{t} \\ \mathbf{r} \end{bmatrix}, \tag{B.5}$$

where **t** and **r** are respectively the translation and the rotation of the platform. **t** and **r** have to be intended as 'small' (infinitesimal) displacements.

According to the static analysis [10, 19], when the external wrench is applied on the platform of a 3-UPU TPM, the i^{th} leg is loaded by a torque m_{ti}, $i = 1, 2, 3$, by an axial forces f_i, $i = 1, 2, 3$, and a pure bending moment m_{bi}, $i = 1, 2, 3$. The rate bending/torque (m_{bi}/m_{ti}) on the i^{th} leg is small (≤ 0.3) in the whole workspace when the axes of the revolute joints of the base and the platform respectively are coplanar [27]. For this reason, the bending moment m_{bi} will be ignored.

In order to define the matrix **H**, the following procedure is adopted. For a given input of the actuators, the 3-UPU TPM becomes a structure. Each leg can be considered as a serial chain of type UU, because the actuated prismatic pair variable is given.

Due to the torque m_{ti} and the axial force f_i, $i = 1, 2, 3$, the i^{th} leg undergoes a torsion and an axial deformation. Figure 14 depicts the elastic model of the 3-UU structure, where k_{ri} and k_{ai} represent the torsional and axial stiffnesses of the i^{th} leg and the base and platform U joints are not represented for simplicity (the platform, the base and the universal joints are considered as rigid, while the legs as deformable).

In order to consider the displacement of the platform produced by the deformation of the leg links due to the torque and to the axial force, additional elastic pairs are introduced for each leg. Namely: a revolute pair with the axis directed as the torque axis and a prismatic pair directed as the unit vector of the leg $\mathbf{s}_i$, which can model respectively the torsional and the axial elastic deformation of the leg, given by θ^i_3 and d^i_4 respectively, Fig.15 shows this for the leg 1. An equivalent manipulator is thus defined, as represented in Fig. 15, which allows a general displacement of the platform (in 3D Cartesian space) that can be expressed as a function of the six variables θ^i_3 and d^i_4, $i = 1, 2, 3$. Therefore the equivalent mechanism can model the influence of a platform displacement on the θ^i_3 and d^i_4 variables.

The procedure to find the stiffness matrix **H** is composed of five steps.

The first one is to express the pose of the reference system S_p fixed to the platform with origin at point O_p with respect to system S_b itself. In other words, to determine the 4×4 matrices ($\mathbf{N}^i$, $i = 1, 2, 3$) which transform the homogenous coordinates of a point from S_p to S_b.

For the i^{th} leg, the 4×4 matrix $\mathbf{N}^i$ can be expressed as the product of the 4×4 matrices $\mathbf{C}_j^i$, $j = 0, ..., 6$, which transform the homogenous coordinates of a point from the system S_j (attached to the link j–1) to the system S_{j+1} (attached to the link j), $j = 0, ..., 6$, (S_0 and S_7 correspond respectively to S_b and S_p as shown in Fig. 15, which shows a schematic of the leg 1). The systems S_j, $j = 1, ..., 6$, are defined according to the Denavit-Hartenberg (D-H) notation [28]. Each matrix $\mathbf{C}_j^i$ is a function of the corresponding variable of motion between link j–1 and link j. Therefore the matrix $\mathbf{N}^i$ is a function of the joint variables θ^i_1, θ^i_2, θ^i_3, d^i_4, θ^i_5, θ^i_6. The matrix $\mathbf{N}^i$ is then given by:

$$\mathbf{N}^i\left(\theta_1^i,\ \theta_2^i,\ \theta_3^i,\ d_4^i,\ \theta_5^i,\ \theta_6^i\right)=\prod_{j=0}^{6}\mathbf{C}_j^i,\quad i=1,\ 2,\ 3. \tag{B.6}$$

For instance, based on the schematic of Fig. 15, the D-H parameters for the leg 1 can be obtained. They are reported in Table 6.

According to Eqn. (B.5), it can be seen that the first column of the stiffness matrix **H** corresponds to the vector of force and moment applied at the reference point O_p when a platform translation of one unit along the x axis of the reference system S_b is performed.

Then, the second step is to find the six variables θ^i_3 and d^i_4, $i = 1, 2, 3$, which characterize respectively the torsion and the axial deformation of the i^{th} leg ($i = 1, 2, 3$) when a platform translation of one unit along the x axis of the reference system S_b is performed. In general, the homogeneous matrix $\mathbf{\Sigma}$ which directly transforms the homogenous coordinates of a point from S_p to S_b can be written as follows [29]:

$$\mathbf{\Sigma}=\left[\sigma_{ij}\right]\qquad i,j=1,\ 2,\ ...,\ 4 \tag{B.7}$$

with:

$$\sigma_{11} = c\varphi_2\, c\varphi_3;\ \ \sigma_{12} = -c\varphi_2\, sc\varphi_3;\ \ \sigma_{13} = s\varphi_2;\ \ \sigma_{14} = x+\Delta x;\ \ \sigma_{21} = s\varphi_1\, s\varphi_2\, c\varphi_3 + c\varphi_1\, s\varphi_3;$$
$$\sigma_{22} = -\,s\varphi_1\, s\varphi_2\, s\varphi_3 + c\varphi_1\, c\varphi_3;\ \ \sigma_{23} = -\,s\varphi_1\, c\varphi_2;\ \ \sigma_{24} = y+\Delta y;$$
$$\sigma_{31} = -\,c\varphi_1\, s\varphi_2\, c\varphi_3 + s\varphi_1\, s\varphi_3;\ \ \sigma_{32} = c\varphi_1\, s\varphi_2\, s\varphi_3 + s\varphi_1\, c\varphi_3;\ \ \sigma_{33} = c\varphi_1\, c\varphi_2;\ \ \sigma_{34} = z+\Delta z;$$
$$\sigma_{41} = \sigma_{42} = \sigma_{43} = 0;\ \ \sigma_{44} = 1;\ \ \varphi_i = \beta_i+\Delta\beta_i,$$

where c(.) and s(.) stand for the cosine and the sine of the argument; β_1, β_2 and β_3 are the Euler angles about x, y, and z axes respectively; Δx, Δy and Δz are respectively the small translations of the platform along x, y and z axes of S_b; and $\Delta\beta_1$, $\Delta\beta_2$, $\Delta\beta_3$ are respectively the small variations of the Euler angles. Therefore $\Delta\gamma = (\Delta x, \Delta y, \Delta z, \Delta\beta_1, \Delta\beta_2, \Delta\beta_3)^T$ represents a small variation of the displacement of the platform.

For a platform translation of one unit along the x axis of the reference system S_b, that is for $\Delta\gamma = (1,\ 0,\ 0,\ 0,\ 0,\ 0)^T$, the variables θ^i_3 and d^i_4 in the i^{th} leg can be found by solving the following system:

$$\mathbf{N}^i = \mathbf{\Sigma} \quad i = 1, 2, 3. \tag{B.8}$$

Indeed, from system (B.8), six independent equations can be extracted (three from the last column of the matrices and three from the rotational part of the matrices). The equations have six dependent variables (θ^i_1, θ^i_2, θ^i_3, d^i_4, θ^i_5, θ^i_6), for given x, y, and z (coordinate of the point O_p in S_b).

Then, by writing system (B.8) for all three legs, a system of 18 independent equations in 18 variables is obtained, which can be solved for the dependent variables, thus providing the values of θ^i_3 and d^i_4, $i = 1, 2, 3$, for each leg.

The third step is to use the axial, k_{ai}, and the rotational, k_{ri}, stiffnesses of the i^{th} leg in order to compute the value of the force f_i along $\mathbf{s}_i$ and the moment m_i around $\mathbf{u}_i$ respectively related to the rotation θ^i_3 and the translation d^i_4 of the i^{th} leg:

$$f_i = k_{ai} d^i_4, \qquad i = 1, 2, 3, \tag{B.9}$$

$$m_i = \frac{k_{ri}\theta^i_3}{\cos\psi_i}, \qquad i = 1, 2, 3, \tag{B.10}$$

where ψ_i is the angle between the unit vectors $\mathbf{s}_i$ and $\mathbf{u}_i$.

By choosing an annular section of the leg, k_{ai} and k_{ri} can be computed as follows:

$$k_{ai} = \frac{\pi E_i \left(R^2_{ext,i} - R^2_{int,i}\right)}{l_i}, \qquad i = 1, 2, 3, \tag{B.11}$$

$$k_{ri} = \frac{G_i I_{0i}}{l_i}, \qquad i = 1, 2, 3, \tag{B.12}$$

where E_i and G_i are respectively the Young and the Coulomb modules of the i^{th} leg; $R_{ext,i}$ and $R_{int,i}$ are the external and the internal radii of the annular section of the i^{th} leg; I_{0i} is the polar moment of inertia of the i^{th} leg, and l_i is the length of the i^{th} leg.

The fourth step is to use the Eqn.(B.1) to compute the external forces **F** and moments **M**, to be applied at the reference point O_p of the platform for the platform equilibrium, which will correspond to the first column of the stiffness matrix **H**.

The fifth step is to repeat the three previous steps (from the second to the fourth) to compute, analogously to what was done for the first column, the second, the third, the fourth, the fifth and the sixth column of the stiffness matrix **H**. This can be performed by imposing respectively a translation of one unit and a rotation of one unit as well in all and around all directions, that is by imposing

$\mathbf{\Delta\gamma} = (0, 1, 0, 0, 0, 0)^T$, $\mathbf{\Delta\gamma} = (0, 0, 1, 0, 0, 0)^T$, …, $\mathbf{\Delta\gamma} = (0, 0, 0, 0, 0, 1)^T$.

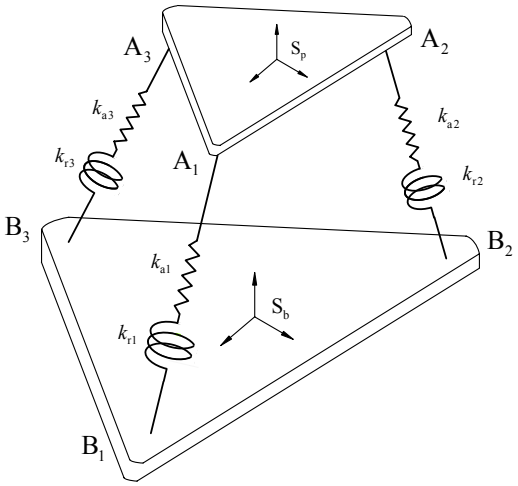

Fig. 14 – Stiffness model of the 3-UPU.

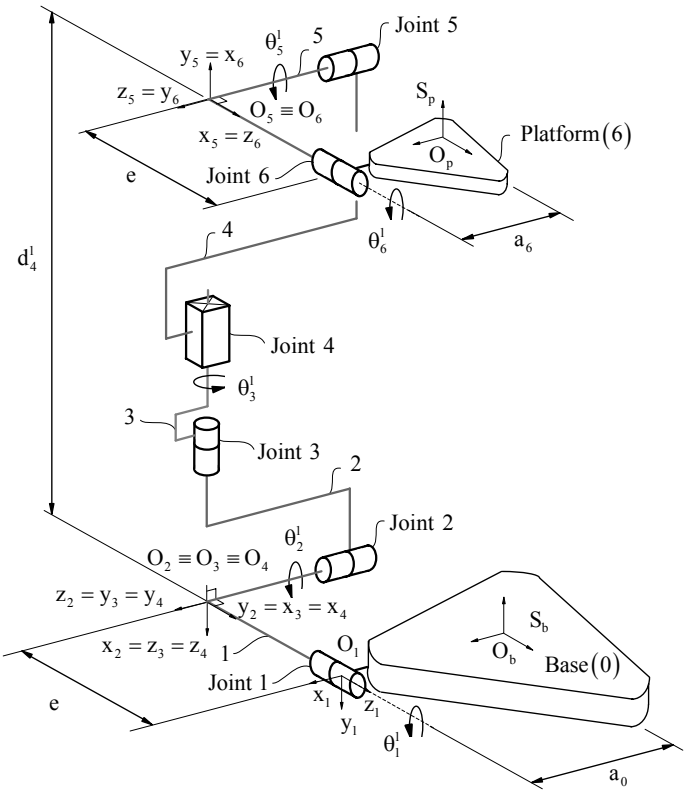

Fig. 15 – Parameters of Denavit-Hartenberg on the leg 1 of the 3-UPU TPM.

At this stage a stiffness index can be defined. The determinant of the stiffness matrix **H** cannot be taken as a stiffness index because it has components which do not have the same units [25]. One of the best alternatives is to take as stiffness indexes T_{sfi} the values of sf_k, $k = 1, 2, 3, 4$, which correspond respectively to the absolute value of the determinants of the four 3×3 matrices $\mathbf{H}_k$, $k = 1, 2, 3, 4$, obtained by partitioning the stiffness matrix computed above [30], and consider them independently; sf_1 and sf_2 represent respectively the stiffness of the manipulator to the translation and the rotation of the platform due to the external force **F**, while sf_3 and sf_4 represent respectively the stiffness of the manipulator to the translation and the rotation of the platform due to the external moment **M**.

Table 6

Denavit-Hartenberg parameters on the leg 1
for the architectures 1.A, 2.A

Link j	θ^i_j	α^i_j	d^i_j	a^i_j
Base (0)	0	$-\pi/2$	0	a_0
1	θ^1_1	$\pi/2$	0	0
2	θ^1_2	$\pi/2$	0	0
3	θ^1_3	0	0	0
4	0	$-\pi/2$	$-d^1_4$	0
5	θ^1_5	$\pi/2$	0	0
Platform (6)	θ^1_6	$\pi/2$	0	$-a_6$

Received on January 4, 2012

REFERENCES

1. CLAVEL, R., *Delta, a fast robot with parallel geometry*, 18th Int. Symp. on *Industrial Robots*, April 26-28, 1988, Lausanne, pp. 91-100.
2. HERVE, J.M., SPARACINO, F., *Structural synthesis of parallel robots generating spatial translation*, 5th ICAR International Conference on *Advanced Robotics*, June 19-22, 1991, Pisa, pp. 808-813.
3. TSAI, L.W., *Kinematics of three-degrees of freedom platform with three extensible limbs*, in *Recent advances in robot kinematics*, Kluwer, Dordrecht, 1972, pp. 93-99.
4. PARENTI-CASTELLI, V., BUBANI, F., *Singularity Loci and Dimensional Design of a Translation 3-dof Fully-Parallel manipulator*, Proceedings of *Advances in Multibody Systems and Mechatronics*, 2000, Duisburg, pp. 319-332.
5. PARENTI-CASTELLI, V., DI GREGORIO, R., *Influence of the manufacturing errors on the kinematic performances of the 3-UPU parallel mechanism*, 2nd Chemnitz Parallel Kinematics seminar – *Working Accuracy of Parallel Kinematics*, 2000, pp. 85-100.
6. DI GREGORIO, R., PARENTI-CASTELLI, V., *Mobility analysis of the 3-UPU parallel mechanism assembled for a pure translational motion*, ASME Transactions, Journal of Mechanical Design, **124**, pp. 259-264, 2002.

7. TSAI, L.W, JOSHI, S., *Kinematics analysis of 3-DOF position mechanisms for use in hybrid kinematic machines*, ASME Transactions, Journal of Mechanical Design, **124**, pp. 245-253, 2002.
8. GOSSELIN, C., ANGELES, J., *The optimum kinematic design of a spherical three-degree-of-freedom parallel manipulator*, ASME Journal of Mechanisms, Transmission and Automation in Design, **111**, pp. 202-207, 1989.
9. DI GREGORIO, R., PARENTI-CASTELLI, V., *Influence of the geometric parameters of the 3-UPU parallel manipulator on the singularity loci Singularity Loci*, International Workshop – *Parallel Kinematic Machines*, Milan, 1999.
10. KONG, X., GOSSELIN, C., *Type Synthesis of 3-DOF Translational Parallel Manipulators Based on Screw Theory*, Journal of Mechanical Design, Transactions of the ASME, **126**, pp. 83-92, 2004.
11. ZLATANOV, D., BONEV, I.A., GOSSELIN, C., *Constraint singularities of parallel mechanisms*, Proceedings – IEEE International Conference on *Robotics and Automation*, 2002, pp. 496-502.
12. GOGU, G., *Structural Synthesis of Parallel Robots – Part 2: Translational Topologies with Two and Three Degrees of Freedom*, Series: Solid Mechanics and Its Applications, Vol. 159, Springer, 2009.
13. CHEBBI, A.H., PARENTI-CASTELLI, V., ROMDHANE, L., *Design of a Pure Translation Manipulator with clearance joints*, 3rd International Congress *Design and Modelling of Mechanical Systems*, March 16-18, 2009, Hammamet.
14. DI GREGORIO, R., PARENTI-CASTELLI, V., *A Translational 3-DOF Parallel Manipulator*, in *Advances in Robot Kinematics: Analysis and Control*, 1998, pp. 49-58.
15. YANG PO-HUA, K., WALDRON, D.E.ORIN., *Kinematic of a three-degree-of-freedom motion platform for a low-cost driving simulator*, in *Advances in Robot Kinematics*, Kluwer Academic Publishers, 1996, pp. 89-98.
16. KONG, X., GOSSELIN, C., *Type Synthesis of Parallel Mechanisms*, Springer London Publisher, 2007.
17. WALTER, D.R., HUSTY, M.L., PFUMER, M., *The SNU 3-UPU Parallel Robot from a Theoretical Viewpoint*, Proceedings of the Second International Workshop on *Fundamental Issues and Future Research Directions for Parallel Mechanisms and Manipulators*, 2008, Montpellier, pp. 1-8.
18. WALTER, D.R., HUSTY, M.L., PFUMER, M., *A Complete Kinematic Analysis of the SNU 3-UPU Parallel Robot*, Contemporary Mathematics, American Mathematical Society, **496**, pp. 331-346, 2009.
19. WOLF, A., SHOHAM, M., *Screw theory tools for the synthesis of the geometry of a parallel robot for a given instantaneous task*, Mechanism and Machine Theory, **41**, pp. 656-670, 2006.
20. CHEBBI, A.H., PARENTI-CASTELLI, V., *Influence of the geometry on the performances of the 3-UPU parallel manipulator*, 3rd European Conference on *Mechanism Science*, September 14-18, 2010, Cluj-Napoca, pp. 595-603.
21. ANGELES, J., *Fundamentals of Robotic Mechanical Systems. Theory, Methods, and Algorithms,* Second Edition, Springer-Verlag, 2002.
22. MA, O., ANGELES, J., *Optimum Architecture Design of Platform Manipulator*, Proc. IEEE Int. Conf. on *Robotics Automat*, 1991, pp. 1131-1135.
23. LI, Y., XU, Q., *Kinematic Analysis and Design of a New 3-DOF Translational Parallel Manipulator*, ASME Transactions, Journal of Mechanical Design, **128**, pp. 729-737, 2006.
24. GOSSELIN, C., ANGELES, J., *A Global Performance Index for the Kinematic Optimization of Robotic Manipulators*, ASME Transactions, Journal of Mechanical Design, **113**, pp. 220-226, 1991.
25. DUFFY, J., *The Fallacy of Modern Hybrid Control Theory that is Based on 'Orthogonal Complements' of twist and Wrench Spaces*, Journal of Robotic Systems, **7**, pp. 139-144, 1990.

26. CHEBBI, A.H., PARENTI-CASTELLI, V., *Potential of the 3-UPU Translational Parallel Manipulator*, Proceeding of ASME 2010 International Design Engineering Technical Conferences – *Computers and Information in Engineering Conference* (IDETC/CIE), August 15-18, 2010, Montreal, pp. 1-11.
27. CHEBBI, A.H., PARENTI-CASTELLI, V., *Analysis of the internal torque and bending moment acting on the legs of the 3-UPU Translational Parallel Manipulator*, 4th Workshop Ettore Funaioli, Bologna, July 18, 2010.
28. HARTENBERG, R.S., DENAVIT, J., *Kinematic synthesis of linkages*, McGraw-Hill Education Publisher, 1964.
29. JOHN, J.C., *Introduction to robotics mechanics and control*, Second Edition, Addison-Wesley Publishing Company, 1989.
30. PASHKEVICH, A., CHABLAT, D, WENGER., P, *Stiffness analysis of overconstrained parallel manipulators*, Mechanism and Machine Theory, **44**, pp. 966-982, 2009.